# NJC

## Accepted Manuscript

This article can be cited before page numbers have been issued, to do this please use: Z. Ku, N. H. Tiep, B. Wu, T. C. Sum, D. Fichou and H. J. Fan, *New J. Chem.*, 2016, DOI: 10.1039/C6NJ00188B.

View Article Online
DOI: 10.1039/C6NJ00188B

New Journal of Chemistry

RSCPublishing

COMMUNICATION

# Solvent engineering for fast growth of centimetric high-quality $CH_3NH_3PbI_3$ perovskite single crystals

Cite this: DOI: 10.1039/x0xx00000x

Zhiliang Ku,[a] Nguyen Huy Tiep,[a,b] Bo Wu,[a] Tze Chien Sum,[a] Denis Fichou,[a,c,d] and Hong Jin Fan.[a,*]

Received 00th January 2012,
Accepted 00th January 2012

DOI: 10.1039/x0xx00000x

www.rsc.org/

**Centimetre-scale $CH_3NH_3PbI_3$ perovskite single crystals of high structural quality are grown by a new versatile method based on the use of a binary solvent mixture at a temperature as low as 70°C. The growth rate is fast enough for a millimeter scale seed crystal to grow to the centimeter scale in a few hours.**

Over the last few years, organo-lead trihalide hybrid perovskites ($CH_3NH_3PbX_3$, X=Cl, Br, I) have generated a tremendous interest in electronic and photonic applications such as solar cells,[1-9] lasing,[10, 11] light-emitting diodes,[12, 13] and photodetectors.[14-16] In particular, perovskite solar cells (PSCs) have now achieved power conversion efficiencies (PCE) up to 20.1%,[9] following a rapid surge of development since PSC devices were first reported in 2009 with an efficiency of 3.8% only.[17] This makes PSCs highly competitive to crystalline silicon and conventional thin film PV technologies using CIGS and CdTe. The success of perovskites in solar cells is mainly due to their superior characteristics including high absorption coefficient,[18] ambipolar transport properties,[19] long carrier diffusion lengths,[20] and low intrinsic recombination rates.[21] Up to now, PSCs are exclusively based on microcrystalline and polycrystalline thin films while single crystal devices remain out of reach due to the difficulty in growing large perovskite single crystals. However, more and more evidences show that grain boundaries, voids and surface defects within the microcrystalline perovskite films act as traps for the charge carriers during solar cell operation, thus leading to reduced PV performances and significant hysteretic effects in J-V curves.[22-25] Therefore, many efforts are being focused on improving the crystalline quality of the films,[26-29] which is expected to reduce the overall bulk defect density and mitigate hysteresis by suppressing charge recombination to finally lead to higher power conversion efficiencies. It is then clear that the availability of large centimeter scale perovskite single crystals could afford maximized device performances in PV cells and other applications.

As early as 1987, it was reported that $CH_3NH_3PbI_3$ single crystals can be synthesized in concentrated aqueous solutions of HI acid containing $Pb^{2+}$ ions and a proportional amount of $CH_3NH_3^+$ ions.[30] Following that method, $CH_3NH_3PbI_3$ large single crystals have been reported in recent years.[31, 32] Since then, other methods based on organic solutions have been developed to grow centimetric $CH_3NH_3PbI_3$ single crystals.[33, 34] The trap density measured in these single-crystalline perovskites is extremely low in the range $10^9$–$10^{10}$ $cm^{-3}$, resulting in a high carrier mobility (164±25 $cm^2$ $V^{-1}$ $s^{-1}$) and long diffusion lengths (>175 μm). These results pave the way toward high-performance PSCs based on wafer-scale single crystalline perovskites.

However, the above crystal growth methods remain strenuous and time-consuming and are not appropriate to large-scale production. Recently, two different research groups observed that, in certain organic solvents, the solubility of $CH_3NH_3PbI_3$ substantially decreases at elevated temperatures.[35, 36] They grew large crystals by dissolving $CH_3NH_3I$ and $PbI_2$ into γ-butyrolactone (GBL) and subsequently heating the solution up to 110°C. We describe here a fast and convenient method to grow high-quality centimetric $CH_3NH_3PbI_3$ single crystals under mild conditions (70°C) by using a novel solvent engineering approach and fully characterized them.

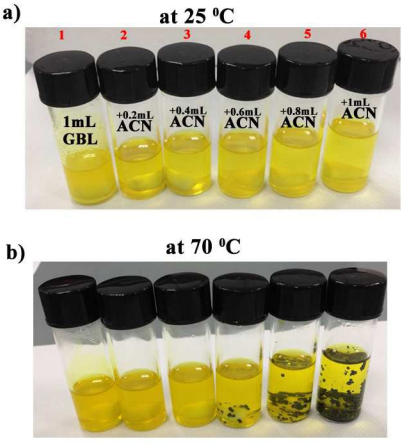


**Fig. 1** Photographs of $CH_3NH_3PbI_3$ precursor solutions with different concentrations of solvents at (a) 25°C and (b) after heating at 70°C.

View Article Online
DOI: 10.1039/C6NJ00158B Journal Name



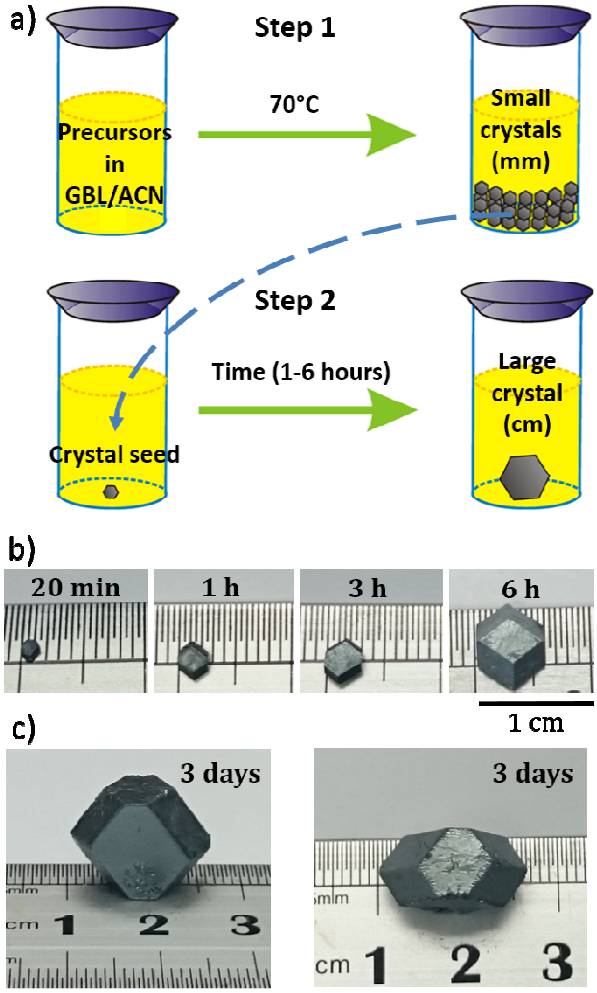


**Fig. 2** a) Schematic of the two-step solvent engineering process for the growth of large $CH_3NH_3PbI_3$ single crystals. b) Photographs of crystals obtained after various growth times (20 min to 6 h). c) Front (left) and side (right) views of a crystal obtained after 3 days (diameter=1.7 cm).

In a first step (Fig. 1a), six flasks are filled with a $CH_3NH_3PbI_3$ precursor solution constituted by 1 mL of GBL (density=1.14 g $mL^{-1}$), 195.5 mg of $CH_3NH_3I$ ($1.23 \times 10^{-3}$ mole) and 572.8 mg of $PbI_2$ ($1.23 \times 10^{-3}$ mole). Then, various volumes of acetonitrile (respectively 0; 0.2; 0.4; 0.6; 0.8; and 1.0 mL) are added into the six successive flasks. After being magnetically stirred at room temperature (25°C) for 1 h, the content of the first flask (without addition of acetonitrile) remains unclear, indicating that both $CH_3NH_3PbI_3$ precursors possess a limited solubility in GBL at 25°C. Interestingly, although the two $CH_3NH_3PbI_3$ precursors have a poor solubility in acetonitrile (ACN),[37] the GBL/ACN binary solvent mixture reveals to be a good solvent and all these solutions look optically clear. When the solutions are heated to 70°C, within 30 minutes small black crystals of $CH_3NH_3PbI_3$ precipitate from the solutions that contain ACN volumes equal or higher than 0.6 mL (Fig. 1b). The number of crystals increases as the added ACN volume increases. We note that the solubility of $CH_3NH_3I$ and $PbI_2$ precursors in GBL/ACN binary solvent mixtures is more sensitive to temperature than in pure GBL (Fig. S1).

In a second step, one tiny black $CH_3NH_3PbI_3$ crystals is picked out from a flask and introduced into a new flask containing a fresh solution of both $CH_3NH_3I$ and $PbI_2$ precursors with similar composition as in step one (Fig. 2). The solution is again heated up to 70°C, thus allowing the crystal seed to further grow in size. By repeating this heat-and-pick process, the $CH_3NH_3PbI_3$ crystals gradually grow into larger sizes (Fig. 2b). It is noteworthy that the crystals prepared by this low-temperature method have a growth rate as fast as along methods reported previously.[35, 36] After only 6 hours their diameter is close to 1 cm to even reach 1.7 cm after 3 days.

X-ray diffraction (XRD) was used to characterize the crystallinity of the as-prepared $CH_3NH_3PbI_3$ crystals. Figure 3 shows the powder XRD patterns of the $CH_3NH_3PbI_3$ powder milled from the large crystals. For comparison, we also calculated the standard pattern of $CH_3NH_3PbI_3$ crystal with pure tetragonal phase (Fig. 3, red pattern). It shows that the main peaks for the as-prepared $CH_3NH_3PbI_3$ are at $2\theta$=14.1°, 28.4° and 40.4° (Fig. 3, black pattern). The position of the main peaks reveal that as-prepared $CH_3NH_3PbI_3$ crystals possess a tetragonal structure. Meanwhile, the clear peaks of (121) and (022) (splitting from the (111) peak of the cubic phase) at $2\theta$=23.5° and $2\theta$=24.5° further confirms that the crystal adopts a tetragonal phase with high crystalline quality.

High-resolution XRD was also used to examine the $CH_3NH_3PbI_3$ single crystal. The $2\theta$ scan results (Fig. 3 blue pattern) show only diffraction peaks from the (112), (020), (224), (040), (336) and (060) planes at $2\theta$ = 19.89°, 19.99° ,40.43°, 40.63° ,62.44° and 62.76°, respectively. These peaks reveal that the as-prepared large $CH_3NH_3PbI_3$ crystal possess a single-crystalline nature. To confirm this, pole figures were measured from one of the $CH_3NH_3PbI_3$ crystal natural facets. The results are in agreement with the pattern expected for the {010} facet, indicating that the <010> plane is parallel to the sample surface. By calculating the Euler angles, we can conclude that this crystal exposes its natural facets {010} and {112} (Fig. S2).

Scanning electron microscopy (SEM) images of one non-perfect crystal (Fig. 4 and S3) show that the surfaces of the crystal is not smooth; some areas are smooth while in other areas, islands and terraces are obviously seen. The tetragonal islands are indicative of a layer-by-layer growth mode of the perovskite crystal. During the simultaneous nucleation and growth of pyramids, tetragonal islands form on the surface of the crystal, and may evolve into truncated tetragonal bipyramids with a dominant (100) plane. The steps and terraces are also seen which can be the boundaries of the growing truncated tetragonal bipyramids.

In order to examine the thermal stability of the $CH_3NH_3PbI_3$ single crystals, we used thermogravimetric analysis (TGA) under nitrogen flow from room temperature up to 600°C (Fig. 5). It has been reported that $CH_3NH_3PbI_3$ thin films decompose at temperatures as low as ≈150°C.[26, 36] In contrast the TGA trace of our perovskite crystals shows no signature of mass loss until 240°C, indicating a higher thermal stability as compare to thin films. Beyond 240°C, the crystals undergo a 20% mass loss of HI, followed by a 6% loss of the $CH_3NH_2$ component at 337°C, indicating a stronger binding of the amine group in the perovskite matrix than HI. At around 385°C and beyond, the inorganic precursor $PbI_2$ is gradually sublimed.

View Article Online
DOI: 10.1039/C6CC04188B COMMUNICATION



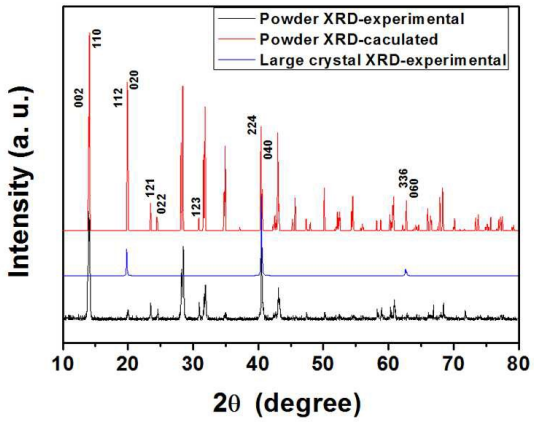


**Fig. 3** XRD patterns recorded on $CH_3NH_3PbI_3$ powder (black) and centimetric single crystals (blue). The red pattern is calculated for the perovskite powder.

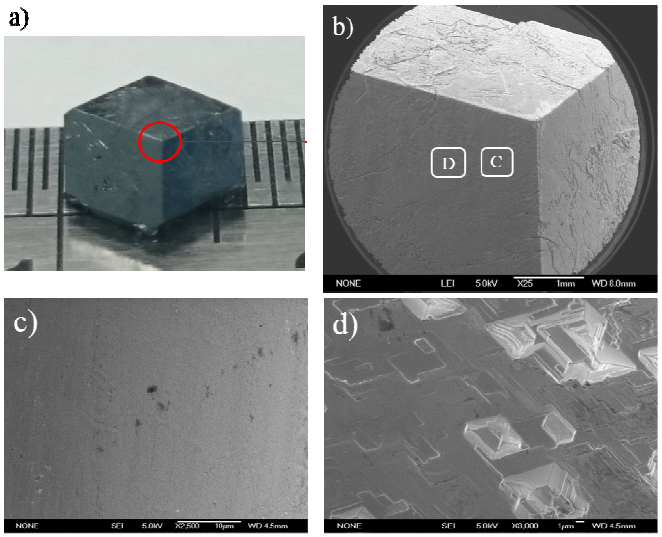


**Fig. 4** Photography (a) and SEM images (b-d) of a non-perfect tetragonal $CH_3NH_3PbI_3$ crystal. SEM images in (c and d) show magnified view of one side faces indicated in (b). Refer Figure S1 for an enlarged view of (b).

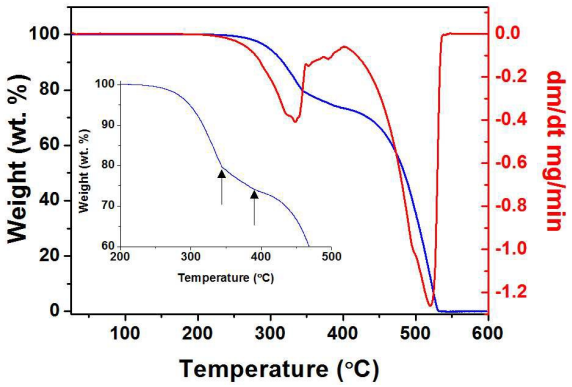


**Fig. 5** Thermal gravimetric analysis (TGA) of the $CH_3NH_3PbI_3$ single crystals.

Finally, the optical properties of the large $CH_3NH_3PbI_3$ crystal were studied by photoluminescence (PL) spectroscopy. As shown in Fig 6a, in comparison with the $CH_3NH_3PbI_3$ thin film, the PL peak position of the large single crystal shows a slight red shift (775 nm for thin film and 783 nm for single crystal). This could indicate a tighter lattice strain in thin film than single crystal.[34] Moreover, the time-dependent PL signals of single crystal and thin film were measured at their respective PL peak wavelengths. Biexponential fitting was performed to determine the carrier dynamics (Fig. 6b). The single crystal exhibited a fast ($\tau$=4.9±0.1 ns) and slower lifetime ($\tau$=57.0±0.7 ns). The fast one is attributed to the carrier recombination lifetime on the surface while the slow one is attributed to that from beneath the surface (in the bulk).[34] Meanwhile, only a fast decay can be observed in the thin film sample ($\tau$=5.1±0.1 ns). The front face of the crystal would then be similar to a thin film where the recombination lifetime is strongly influenced by impurities, surface defects, dangling bonds, thus yielding a faster lifetime of ≈5 ns. The longer recombination lifetime in the bulk of the crystal suggests a greatly reduced trap density as compared to the surface and that of the polycrystalline thin film and is characteristic of the bulk properties of $CH_3NH_3PbI_3$.[33, 34]

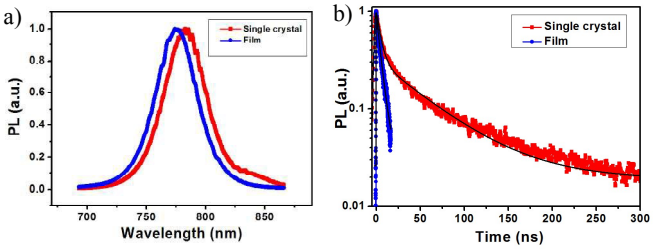


**Fig. 6** (a) Steady-state and (b) time-resolved PL spectra of $CH_3NH_3PbI_3$ thin films and single crystals. Black lines represent calculated fits.

In summary, we succeeded in growing centimetric $CH_3NH_3PbI_3$ perovskite single crystals of high-quality using a convenient novel method based on the use of a ACN/GBL binary solvent mixture at low temperature (70°C). The XRD analysis and SEM images confirm that as-prepared $CH_3NH_3PbI_3$ crystals are single crystals with tetragonal structure. A slow carrier dynamic is observed on the time-dependent PL signals, which reveals the lifetime of carriers propagating deeper in the crystal. Meanwhile, TGA result indicates that the $CH_3NH_3PbI_3$ single crystal possess better thermal stability than the common thin films. Our original solvent engineering method provides new opportunities towards the use of large $CH_3NH_3PbI_3$ single crystals for both fundamental physical studies and technological applications in PV solar cells.

## Acknowledgements

Authors wish to acknowledge the financial supports from the Ministry of Education AcRF grants MOE2011-T3-1-005, MOE2014-T2-1-044 MOE2014-T2-1-132 and Tier 1 grant (RG115/15), as well as SPMS collaborative Research Award M4080536. The Singapore National Research Foundation through the Singapore–Berkeley Research Initiative for Sustainable Energy (SinBeRISE) CREATE Program is also acknowledged.

View Article Online
DOI: 10.1039/C6NJ00188B Journal Name



## Notes and references

[a] *School of Physical and Mathematical Sciences, Nanyang Technological University, 637371, Singapore. Email: FANHJ@ntu.edu.sg*
[b] *Interdisciplinary Graduate School, Nanyang Technological University, 639798, Singapore.*
[c] *CNRS, UMR 8232, Institut Parisien de Chimie Moléculaire, F-75005 Paris, France.*
[d] *Sorbonne Universités, UPMC Univ Paris 06, UMR 8232, Institut Parisien de Chimie Moléculaire, F-75005, Paris, France.*

Z. Ku,and N. H. Tiep contributed equally to this work.

† Electronic Supplementary Information (ESI) available : [Experimental details for perovskite synthesis, thin film deposition, single-crystal X-ray diffraction and solubility measurement]. See DOI: 10.1039/c000000x/

1. H. S. Kim, C. R. Lee, J. H. Im, K. B. Lee, T. Moehl, A. Marchioro, S. J. Moon, R. Humphry-Baker, J. H. Yum, J. E. Moser, M. Gratzel and N. G. Park, *Sci Rep*, 2012, **2**, 591.
2. M. M. Lee, J. Teuscher, T. Miyasaka, T. N. Murakami and H. J. Snaith, *Science*, 2012, **338**, 643-647.
3. J. Burschka, N. Pellet, S. J. Moon, R. Humphry-Baker, P. Gao, M. K. Nazeeruddin and M. Gratzel, *Nature*, 2013, **499**, 316-319.
4. N. J. Jeon, J. H. Noh, W. S. Yang, Y. C. Kim, S. Ryu, J. Seo and S. I. Seok, *Nature*, 2015, **517**, 476-480.
5. M. Liu, M. B. Johnston and H. J. Snaith, *Nature*, 2013, **501**, 395-398.
6. W. Nie, H. Tsai, R. Asadpour, J.-C. Blancon, A. J. Neukirch, G. Gupta, J. J. Crochet, M. Chhowalla, S. Tretiak, M. A. Alam, H.-L. Wang and A. D. Mohite, *Science*, 2015, **347**, 522-525.
7. X. Li, M. Ibrahim Dar, C. Yi, J. Luo, M. Tschumi, S. M. Zakeeruddin, M. K. Nazeeruddin, H. Han and M. Grätzel, *Nat. Chem.*, 2015, **7**, 703-711.
8. H. Zhou, Q. Chen, G. Li, S. Luo, T.-b. Song, H.-S. Duan, Z. Hong, J. You, Y. Liu and Y. Yang, *Science*, 2014, **345**, 542-546.
9. W. S. Yang, J. H. Noh, N. J. Jeon, Y. C. Kim, S. Ryu, J. Seo and S. I. Seok, *Science*, 2015, **348**, 1234-1237.
10. G. Xing, N. Mathews, S. S. Lim, N. Yantara, X. Liu, D. Sabba, M. Grätzel, S. Mhaisalkar and T. C. Sum, *Nat. Mater.*, 2014, **13**, 476-480.
11. H. Zhu, Y. Fu, F. Meng, X. Wu, Z. Gong, Q. Ding, M. V. Gustafsson, M. T. Trinh, S. Jin and X. Y. Zhu, *Nat. Mater.*, 2015, **14**, 636–642.
12. X. Y. Chin, D. Cortecchia, J. Yin, A. Bruno and C. Soci, *Nat. Commun.*, 2015, **6**, 7383.
13. S. D. Stranks and H. J. Snaith, *Nat Nano*, 2015, **10**, 391-402.
14. X. Hu, X. Zhang, L. Liang, J. Bao, S. Li, W. Yang and Y. Xie, *Adv. Funct. Mater.*, 2014, **24**, 7373–7380.
15. S. Zhuo, J. Zhang, Y. Shi, Y. Huang and B. Zhang, *Angew. Chem. Int. Ed.*, 2015, **54**, 5693-5696.
16. H. Deng, D. Dong, K. Qiao, L. Bu, B. Li, D. Yang, H.-E. Wang, Y.-B. Cheng, Z. Zhao, J. Tang and H. Song, *Nanoscale*, 2015, **7**, 4163-4170.
17. A. Kojima, K. Teshima, Y. Shirai and T. Miyasaka, *J. Am. Chem. Soc.*, 2009, **131**, 6050-6051.
18. J. H. Im, C. R. Lee, J. W. Lee, S. W. Park and N. G. Park, *Nanoscale*, 2011, **3**, 4088-4093.
19. E. Edri, S. Kirmayer, A. Henning, S. Mukhopadhyay, K. Gartsman, Y. Rosenwaks, G. Hodes and D. Cahen, *Nano Lett.*, 2014, **14**, 1000-1004.
20. G. Xing, N. Mathews, S. Sun, S. S. Lim, Y. M. Lam, M. Gratzel, S. Mhaisalkar and T. C. Sum, *Science*, 2013, **342**, 344-347.
21. C. Wehrenfennig, G. E. Eperon, M. B. Johnston, H. J. Snaith and L. M. Herz, *Adv. Mater.*, 2014, **26**, 1584-1589.
22. D. W. deQuilettes, S. M. Vorpahl, S. D. Stranks, H. Nagaoka, G. E. Eperon, M. E. Ziffer, H. J. Snaith and D. S. Ginger, *Science*, 2015, **348**, 683-686.
23. G.-J. A. H. Wetzelaer, M. Scheepers, A. M. Sempere, C. Momblona, J. Ávila and H. J. Bolink, *Adv. Mater.*, 2015, **27**, 1837-1841.
24. J. Kim, S.-H. Lee, J. H. Lee and K.-H. Hong, *J. Phys. Chem. Lett.*, 2014, **5**, 1312-1317.
25. H.-S. Kim and N.-G. Park, *J. Phys. Chem. Lett.*, 2014, **5**, 2927-2934.
26. A. Dualeh, N. Tétreault, T. Moehl, P. Gao, M. K. Nazeeruddin and M. Grätzel, *Adv. Funct. Mater.*, 2014, **24**, 3250-3258.
27. Z. Xiao, Q. Dong, C. Bi, Y. Shao, Y. Yuan and J. Huang, *Adv. Mater.*, 2014, **26**, 6503–6509.
28. X. Zheng, B. Chen, C. Wu and S. Priya, *Nano Energy*, 2015, **17**, 269-278.
29. Y. Zhou, M. Yang, A. L. Vasiliev, H. F. Garces, Y. Zhao, D. Wang, S. Pang, K. Zhu and N. P. Padture, *J. Mater. Chem. A*, 2015, **3**, 9249-9256.
30. A. Poglitsch and D. Weber, *J. Chem. Phys.*, 1987, **87**, 6373-6378.
31. T. Baikie, Y. Fang, J. M. Kadro, M. Schreyer, F. Wei, S. G. Mhaisalkar, M. Graetzel and T. J. White, *J. Mater. Chem. A*, 2013, **1**, 5628.
32. Y. Dang, Y. Liu, Y. Sun, D. Yuan, X. Liu, W. Lu, G. Liu, H. Xia and X. Tao, *CrystEngComm*, 2015, **17**, 665-670.
33. Q. Dong, Y. Fang, Y. Shao, P. Mulligan, J. Qiu, L. Cao and J. Huang, *Science*, 2015, **347**, 967-970.
34. D. Shi, V. Adinolfi, R. Comin, M. Yuan, E. Alarousu, A. Buin, Y. Chen, S. Hoogland, A. Rothenberger, K. Katsiev, Y. Losovyj, X. Zhang, P. A. Dowben, O. F. Mohammed, E. H. Sargent and O. M. Bakr, *Science*, 2015, **347**, 519-522.
35. M. I. Saidaminov, A. L. Abdelhady, B. Murali, E. Alarousu, V. M. Burlakov, W. Peng, I. Dursun, L. Wang, Y. He, G. Maculan, A. Goriely, T. Wu, O. F. Mohammed and O. M. Bakr, *Nat. Commun.*, 2015, **6**.
36. Y. Liu, Z. Yang, D. Cui, X. Ren, J. Sun, X. Liu, J. Zhang, Q. Wei, H. Fan, F. Yu, X. Zhang, C. Zhao and S. Liu, *Adv. Mater.*, 2015, **27**, 5176-5183.
37. L. Dou, A. B. Wong, Y. Yu, M. Lai, N. Kornienko, S. W. Eaton, A. Fu, C. G. Bischak, J. Ma, T. Ding, N. S. Ginsberg, L.-W. Wang, A. P. Alivisatos and P. Yang, *Science*, 2015, **349**, 1518-1521.

View Article Online
DOI: 10.1039/C6NJ00188B

# TOC entry

NJ-LET-01-2016-000188

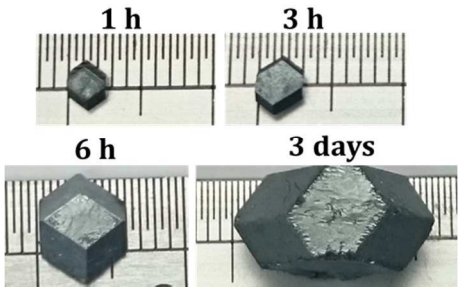


Single crystals of size up to 1.7 centimeter are grown at 70°C in a GBL/ACN binary solvent mixture.